Am J Physiol Endocrinol Metab 294: E345–E351, 2008.
First published December 11, 2007; doi:10.1152/ajpendo.00456.2007.

Angiotensin II-induced skeletal muscle insulin resistance mediated by NF-κB activation via NADPH oxidase

Yongzhong Wei,[1,2] James R. Sowers,[1,2] Suzanne E. Clark,[1,2] Wenhan Li,[1,2] Carlos M. Ferrario,[3] and Craig S. Stump[4,5]

[1]*Department of Internal Medicine, University of Missouri-Columbia;* [2]*Harry S. Truman Memorial Veterans Affairs Medical Center, Columbia, Missouri;* [3]*Wake Forest University School of Medicine, Winston-Salem, North Carolina;* [4]*Diabetes Research Program, Department of Medicine, University of Arizona; and* [5]*Southern Arizona Veterans Affairs Health Care System, Tucson, Arizona*

Submitted 16 July 2007; accepted in final form 7 December 2007

Wei Y, Sowers JR, Clark SE, Li W, Ferrario CM, Stump CS. Angiotensin II-induced skeletal muscle insulin resistance mediated by NF-κB activation via NADPH oxidase. *Am J Physiol Endocrinol Metab* 294: E345–E351, 2008. First published December 11, 2007; doi:10.1152/ajpendo.00456.2007.—Reduced insulin sensitivity is a key factor in the pathogenesis of type 2 diabetes and hypertension. Skeletal muscle insulin resistance is particularly important for its major role in insulin-mediated glucose disposal. Angiotensin II (ANG II) is integral in regulating blood pressure and plays a role in the pathogenesis of hypertension. In addition, we have documented that ANG II-induced skeletal muscle insulin resistance is associated with generation of reactive oxygen species (ROS). However, the linkage between ROS and insulin resistance in skeletal muscle remains unclear. To explore potential mechanisms, we employed the transgenic TG(mRen2)27 (Ren-2) hypertensive rat, which harbors the mouse renin transgene and exhibits elevated tissue ANG II levels, and skeletal muscle cell culture. Compared with Sprague-Dawley normtensive control rats, Ren-2 skeletal muscle exhibited significantly increased oxidative stress, NF-κB activation, and TNF-α expression, which were attenuated by in vivo treatment with an angiotensin type 1 receptor blocker (valsartan) or SOD/catalase mimetic (tempol). Moreover, ANG II treatment of L6 myotubes induced NF-κB activation and TNF-α production and decreased insulin-stimulated Akt activation and GLUT-4 glucose transporter translocation to plasma membranes. These effects were markedly diminished by treatment of myotubes with valsartan, the antioxidant *N*-acetylcysteine, NADPH oxidase-inhibiting peptide (gp91 ds-tat), or NF-κB inhibitor (MG-132). Similarly, NF-κB p65 small interfering RNA reduced NF-κB p65 subunit expression and nuclear translocation and TNF-α production but improved insulin-stimulated phosphorylation (Ser^{473}) of Akt and translocation of GLUT-4. These findings suggest that NF-κB plays an important role in ANG II/ROS-induced skeletal muscle insulin resistance.

nuclear factor-κB; reduced nicotinamide adenine dinucleotide phosphate; renin-angiotensin system; reactive oxygen species; TG(mRen2)27 rat; tumor necrosis factor-α, angiotensin receptor blocker

THE METABOLIC SYNDROME, which is closely associated with obesity, dyslipidemia, hypertension, and type 2 diabetes mellitus, affects 47 million people, or 24% of the US adult population (8, 23, 26). Although insulin resistance is a key factor in the pathogenesis of the metabolic syndrome, skeletal muscle is particularly important in the development of insulin resistance, since it is responsible for ~75–95% of insulin-mediated glucose disposal (26). Skeletal muscle insulin signaling involves insulin binding to its receptor and, subsequently, a series of postreceptor phosphorylation events, including the activation of Akt (protein kinase B) (24). Therefore, factors, such as angiotensin II (ANG II), that impair this signaling processes cause insulin resistance and contribute to systemic glucose intolerance (2, 16, 28).

The renin-angiotensin system (RAS) plays a vital role in regulating blood pressure and the pathogenesis of hypertension and cardiovascular disease. Recent evidence indicates that inhibition of RAS not only improves cardiovascular outcomes but may have metabolic benefits as well; e.g., angiotensin-converting enzyme inhibitors or ANG II type 1 receptor (AT_1R) blockers increase insulin sensitivity (3, 9, 29, 31) and reduce onset of type 2 diabetes mellitus compared with other antihypertensive agents (25). Adverse effects of the RAS appear to act directly on skeletal muscle, since interstitial infusion of ANG II has been shown to induce insulin resistance that is independent of vascular effects, whereas ANG II also impairs insulin signaling in cultured myotubes (19, 30). ANG II has prooxidant effects, in that it induces generation of reactive oxygen species (ROS). We have shown that ROS mediate ANG II-induced skeletal muscle insulin resistance and glucose intolerance in the transgenic TG(mRen2)27 (Ren-2) hypertensive rat, which harbors the mouse renin gene and exhibits elevated tissue ANG II levels (3). Yet the intermediate steps linking ROS to insulin resistance in skeletal muscle remain unknown. It is known that ROS activates multiple transcription factors, including NF-κB (10, 13). NF-κB activation is involved in high-fat diet-induced liver insulin resistance in mice (5). However, it has not been determined whether ANG II activates skeletal muscle NF-κB, thereby providing a potential mechanism for ANG II-induced insulin resistance. In the present study, we employed Ren-2 rats and ANG II-treated myotubes to determine the role of ROS-mediated NF-κB activation in blunting insulin effects on skeletal muscle. Our results suggest that ANG II-induced ROS generation via NADPH oxidase activates NF-κB, which in turn contributes to skeletal muscle insulin resistance.

MATERIALS AND METHODS

Materials. Antibodies against 4-hydroxy-2-nonenal (4-HNE), TNF-α, NF-κB p65, IκBα, Akt, phosphorylated (Ser^{473}) Akt, and

Address for reprint requests and other correspondence: C. S. Stump, Diabetes Research Program, Dept. of Medicine, PO Box 245218, Univ. of Arizona, Tucson, AZ 85724 (e-mail: cstump@deptofmed.arizona.edu).

The costs of publication of this article were defrayed in part by the payment of page charges. The article must therefore be hereby marked "*advertisement*" in accordance with 18 U.S.C. Section 1734 solely to indicate this fact.

glucose transporters (GLUT-4 and GLUT-1) were obtained from Santa Cruz Biotechnology (Santa Cruz, CA), Upstate Signaling Technology (Beverly, MA), Abcam (Cambridge, MA), and Cell Signaling (Beverly, MA); antibody against the Na-K-ATPase α_1-subunit from Upstate Biotechnology (Lake Placid, NY); rat TNF-α ELISA detection kit from R & D Systems (Minneapolis, MN); NF-κB NoShift assay kit from Novagen, EMD Biosciences (San Diego, CA); ANG II, human insulin, and NADPH from Sigma (St. Louis, MO); and DMEM, FBS, and antibiotic-antimycotic solution (10,000 U/ml penicillin G, 10 mg/ml streptomycin, and 25 mg/ml amphotericin B) from GIBCO Invitrogen. The peptide gp91 ds-tat is a generous gift from Dr. Patrick Pagano (Henry Ford Research Institute and Hospital, Detroit, MI), and the scrambled small interfering RNA (siRNA) as control was purchased from Bio-Synthesis (Lewisville, TX) with or without a fluorescent tag (carboxytetramethylrhodamine).

Animals and treatments. Male Ren-2 and Sprague-Dawley (SD) rats were received at 5–6 wk of age from Bowman Gray School of Medicine (Wake Forest University, Winston-Salem, NC). Animal protocols were reviewed and approved by the Harry S. Truman Veterans Affairs Medical Center Animal Care Committee. After a short period of adaptation, Ren-2 rats were randomly assigned to treatment with the AT_1R blocker valsartan (RV group; 30 $mg \cdot kg^{-1} \cdot day^{-1}$) or the SOD/catalase mimetic tempol (RT group; 1 mM) in their drinking water for 21 days or remained untreated (RC group). These animals were compared with age-matched, untreated SD rats. The rats were weighed and anesthetized with pentobarbital sodium (Nembutal, 35 mg/kg ip), and soleus muscles were dissected and trimmed and frozen in liquid nitrogen and stored at −80°C, fixed, or homogenized for further analysis (see below).

Cell culture. L6 rat skeletal muscle cells (American Type Culture Collection) were grown in DMEM with 10% (vol/vol) FBS and 1% (vol/vol) antibiotic-antimycotic solution at 5% CO_2 and 37°C until they reached ~80% confluence. To induce differentiation, cells were further cultured in DMEM containing 2% FBS for 6–8 days. Cells were fed fresh medium every 48 h and used at the myotube stage (60–70%), when GLUT-4 expression is highest (11). Myogenic differentiation to myotubes was confirmed by light microscopy with morphological alignment, elongation, and fusion.

Transfection of gp91 ds-tat. In selected experiments, the NAD(P)H oxidase inhibitor gp91 ds-tat and the scrambled gp91 ds-tat as a control (Bio-Synthesis, Lewisville, TX) were used. The peptide gp91 ds-tat is linked to a nine-amino acid peptide contained in human immunodeficiency virus viral coats (HIV-tat) that is internalized by all cells. The peptide interferes with the binding of the cytosolic subunit $p47^{phox}$ with the membrane subunit $gp91^{phox}$ (Nox2) and inhibits NADPH oxidase activation (18, 32). A scrambled nine-amino acid Nox2 sequence (scramb-tat) was used as a control. In some experiments, gp91 ds-tat and scramb-tat were dissolved in 0.01 mmol/l acetic acid in saline. Myotubes were incubated with gp91 ds-tat (20 μmol/l) or scramb-tat (20 μmol/l) for 1 h before ANG II incubation.

NF-κB p65 siRNA transfection. L6 myotubes were transfected with NF-κB p65 siRNA or control siRNA (Santa Cruz Biotechnology) as described elsewhere (30). The differentiation medium was changed to antibiotic-free medium on *day 4*, and 0.6 μg of siRNA was added to the transfection medium. At 6 h after transfection, DMEM containing 4% FBS was added to each well to a final concentration of 2% FBS (vol/vol). Cells were transfected again on *day 6* with 1 μg of siRNA. At 6 h after transfection, the cells were further incubated with ANG II for an additional 24 h. In some experiments, the cells were stimulated with insulin for 30 min.

Measurement of NF-κB activation. Skeletal muscles were dissected and weighed, homogenized in 6 vol of ice-cold buffer [10 mmol/l HEPES (pH 7.9), 100 mmol/l KCl, 0.1 mmol/l EDTA, 0.1 mmol/l EGTA, 0.1 mmol/l dithiothreitol, and 1 mmol/l phenylmethylsulfonyl fluoride] using a Duall homogenizer. The homogenates were centrifuged at 500 *g* for 30 min at 4°C. The supernatant was resuspended in NucBuster reagent, vortexed twice during incubation on ice for 5 min, centrifuged at 16,000 *g* for 5 min at 4°C, and washed with ice-cold PBS (7). L6 myotubes were rinsed with PBS and lysed using lysis buffer as described above. Nuclear fragments were extracted according to the manufacturer's instructions. Nuclear extract (5 μl) was mixed with 15 μl of 4× NoShift bind buffer [poly(dI-dC)·poly(dI-dC), salmon sperm DNA, and wild-type DNA] and incubated for 30 min on ice. Thereafter, 1× NoShift bind buffer (80 μl) was added to each NoShift reaction. The streptavidin plate was washed three times for 5 min with 200 μl of 11× NoShift wash buffer. Reaction solution (100 μl) was dispensed into wells of the freshly washed streptavidin plate, which was sealed with aluminum foil and incubated for 60 min at 37°C. After the washing steps, primary antibody (100 μl) was added to each well, and the sample was incubated for 60 min at 37°C. The sample was incubated in horseradish peroxidase (HRP)-conjugated secondary antibody (1:1,000) for 30 min at 37°C and then in the substrate trimethoxybenzoate for 15 min in the dark at room temperature. Thereafter, 100 μl of 1 N HCl were mixed into each well, and absorbance at 450 nm was measured using a plate reader spectrophotometer (model EL808, Bio-Tek).

TNF-α immunofluorescence. Soleus muscle paraffin cross sections (5 μm) were cut for TNF-α staining. After they were dewaxed, the slides were blocked with 5% rabbit serum containing 1% BSA and 0.1% saponin. Then the slides were incubated with anti-TNF-α (1:200 dilution) overnight at 4°C. After three washes in PBS, rabbit anti-goat IgG antibody conjugated with Alexis 468 (Molecular Probes) was added for 1 h at room temperature. The sections were extensively washed in PBS and mounted on glass slides with mounting medium (Vector), and images were acquired with a fluorescence microscope (Eclipse 50i, Nikon) using Meta Imaging software (Molecular Devices).

Western blot. L6 myotubes were treated with ANG II (10^{-7} M) for 24 h in the absence or presence of losartan (10^{-6} M), *N*-acetylcysteine (NAC, 30 mM), or gp91 ds-tat (20 μM). Then, in some experiments, myotubes were stimulated with insulin (100 nM) for 15 min. Subcellular fractionation of myotubes was performed as previously described (30). Briefly, the myotubes were homogenized in homogenization buffer. The homogenate was centrifuged at 1,000 *g* for 30 min at 4°C. An aliquot of the supernatant (S1, as total homogenate) was frozen and stored at −80°C, and the remaining S1 was centrifuged at 12,000 *g* for 20 min at 4°C, yielding a pellet (mitochondria) and supernatant (S2). S2 was centrifuged at 30,000 *g* for 1 h at 4°C. The pellet containing the Golgi and sarcoplasmic reticulum was discarded, and the supernatant (S3) was centrifuged at 100,000 *g* to enrich the plasma membrane (PM) fraction in the pellet and separate the cytosolic fraction (supernatant). Protein concentrations were determined by the method of Bradford (Bio-Rad reagent). Protein (40 μg) from S2 was loaded in 10% SDS-PAGE gel and probed with rabbit anti-Akt or phosphorylated (Ser^{473}) Akt (1:1,000 dilution) antibodies. Forty micrograms of PM-enriched fraction and total homogenate (S2) protein were subjected to 10% SDS-PAGE and immunoblotted using rabbit anti-GLUT-4 (1:1,000 dilution in 5% milk-TBS). PM enrichment was confirmed by Na-K-ATPase α_1-subunit immunoblotting. An HRP-coupled secondary anti-rabbit IgG antibody was applied and reacted with enhanced chemiluminescence reagent (Amersham Life Science). The membranes were read and quantified with the Bio-Rad Molecular Imager FX Pro Plus MultiImager System. β-Actin was used as a loading control.

Measurement of 4-HNE. 4-HNE, a by-product of lipid peroxidation and marker of oxidative stress, was measured by immunofluorescence staining and Western blot using anti-4-HNE antibody. Paraffin sections (5 μm) of the soleus muscle were microwaved for 10 min for antigen retrieval and incubated with monoclonal mouse antibody against 4-HNE (OXIS) overnight at 4°C. Goat anti-mouse IgG antibody conjugated with Alexis 568 (Molecular Probe) was used as secondary antibody. The images were acquired with a laser-scanning confocal microscope (model IX70, Olympus). Soleus muscle was also homogenized on ice in homogenization buffer [50 mM phosphate

buffer, 0.01 mM EDTA, 1 mM phenylmethylsulfonyl fluoride, 2 μM leupeptin, and 2 μM pepstatin A (pH 7.4)] using a Duall homogenizer. The homogenate was centrifuged at 1,000 *g* for 30 min at 4°C, and the supernatant (S1) was further centrifuged at 13,000 *g* for 20 min at 4°C, yielding supernatant (S2) and a pellet containing mitochondria. Forty micrograms of protein (S2) were loaded in SDS-PAGE gel and probed with primary antibodies (1:1,000 dilution) against 4-HNE-modified proteins. After the membrane was washed, it was incubated with HRP-conjugated secondary antibodies (1:10,000 dilution). The intensities of the immunoblot lanes were quantified using Quantity One software (Bio-Rad). β-Actin was used as a loading control.

RT-PCR amplification. TNF-α mRNA expression was measured by RT-PCR using the following primers: TGGCCCAGACCCTCACACTC (forward) and CTCCTGGTATGAAATGGCAAATC (reverse). For determination of the relative initial amounts of TNF-α cDNA, the cDNA sample was serially diluted 1:5 and 1:25. GAPDH was used as a housekeeping gene to verify that the same amount of RNA was amplified. The PCR products were analyzed using a digital imaging system (Kodak).

TNF-α ELISA. L6 myotubes were stimulated with 10^{-9}–10^{-5} mM ANG II, with and without inhibitors (see Fig. 4), for 24 h. Media samples were collected and centrifuged at 1,000 *g* for 30 min. TNF-α was determined in supernatants using ELISA according to the manufacturer's instruction (R & D Systems).

Statistical analysis. Values are means ± SE from at least three different experiments. One-way ANOVA or Student's *t*-test was used to determine the significance between groups. When an ANOVA *F*-test indicated significance, a protected Fisher's least significant difference post hoc analysis was performed. $P < 0.05$ was considered to be statistically significant.

RESULTS

Increased oxidative stress in soleus muscle from Ren-2 rats. Using a lucigenin assay, we showed that ANG II increases ROS formation in soleus muscle from Ren-2 rats (3) and L6 myotubes (30). ROS are short-lived molecules that exert local effects, such as increased formation of aldehyde by-products, including 4-HNE, which have longer half-lives than ROS (4, 6). Therefore, 4-HNE is considered to be a reliable index of the deleterious effects of ROS on various cellular components, including membranes, proteins, and DNA (4). Western blot analysis and immunohistochemistry have been used to detect modified proteins by 4-HNE (15). In the present study, 4-HNE staining on Western blot was more intense in soleus muscles from Ren-2 (RC) than SD (194%) rats (Fig. 1*A*). When Ren-2 rats were treated with valsartan (RV) or tempol (RT), 4-HNE was significantly reduced compared with untreated RC rats (Fig. 1*A*). Similarly, immunofluorescent staining of soleus muscle sections showed greater 4-HNE accumulation in Ren-2 rats than SD controls and a reduction of 4-HNE staining intensity by valsartan or tempol (Fig. 1*B*).

Increased NF-κB activation in soleus muscle from Ren-2 rats. Oxidative stress activates multiple redox signaling pathways, including NF-κB (13). To test whether increased oxidative stress induced by ANG II was associated with NF-κB activation in Ren-2 skeletal muscle, nuclear fractions were isolated and NF-κB p65 nuclear translocation was determined by NoShift assay. NF-κB p65 nuclear translocation was significantly increased by 189% in soleus muscles from Ren-2 compared with SD rats (Fig. 2*A*). However, NF-κB p65 nuclear translocation was greatly attenuated in muscle from Ren-2 rats treated with valsartan or tempol. Under these conditions, NF-κB activation was significantly correlated ($r = 0.786$, $P < 0.01$) to 4-HNE levels in rat skeletal muscle (Fig. 2*B*). Moreover, decreased levels of cytosolic IκBα were detected in Ren-2 skeletal muscle, whereas valsartan or tempol reversed this effect (Fig. 2*C*).

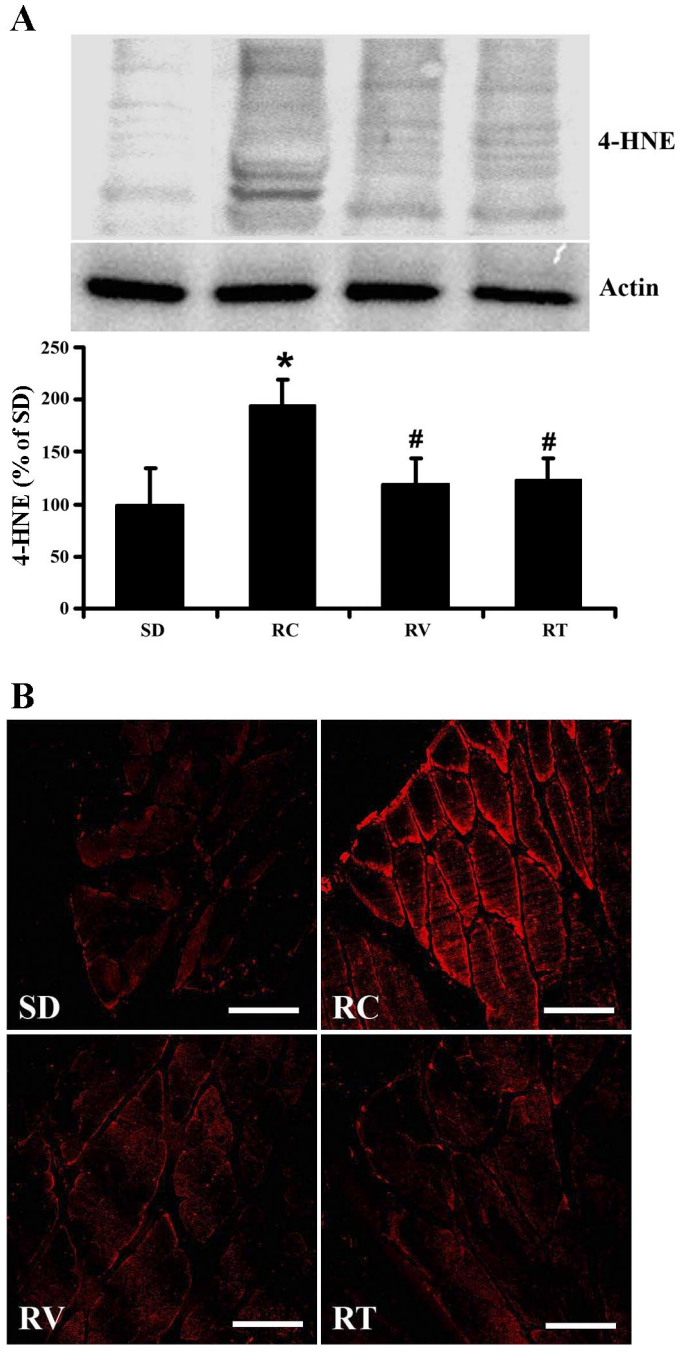

Fig. 1. Oxidative stress marker 4-hydroxy-2-nonenol (4-HNE) in rat skeletal (soleus) muscle shown by immunostaining and Western blot. SD, Sprague-Dawley rats; RC, TG(mRen2)27 (Ren-2) control rats; RV, Ren-2 rats treated with valsartan; RT, Ren-2 rats treated with tempol. *A*: representative immunoblot for 4-HNE (*top*) and summary of lane densitometry from multiple experiments (*bottom*; $n = 4$–5 per group). *$P < 0.05$ vs. SD. #$P < 0.05$ vs. RC. *B*: representative photomicrographs showing increased 4-HNE immunostaining (red) in Ren-2 compared with SD soleus muscle; increase was attenuated in RV and RT groups. Magnification ×400. Scale bar 50 μm.

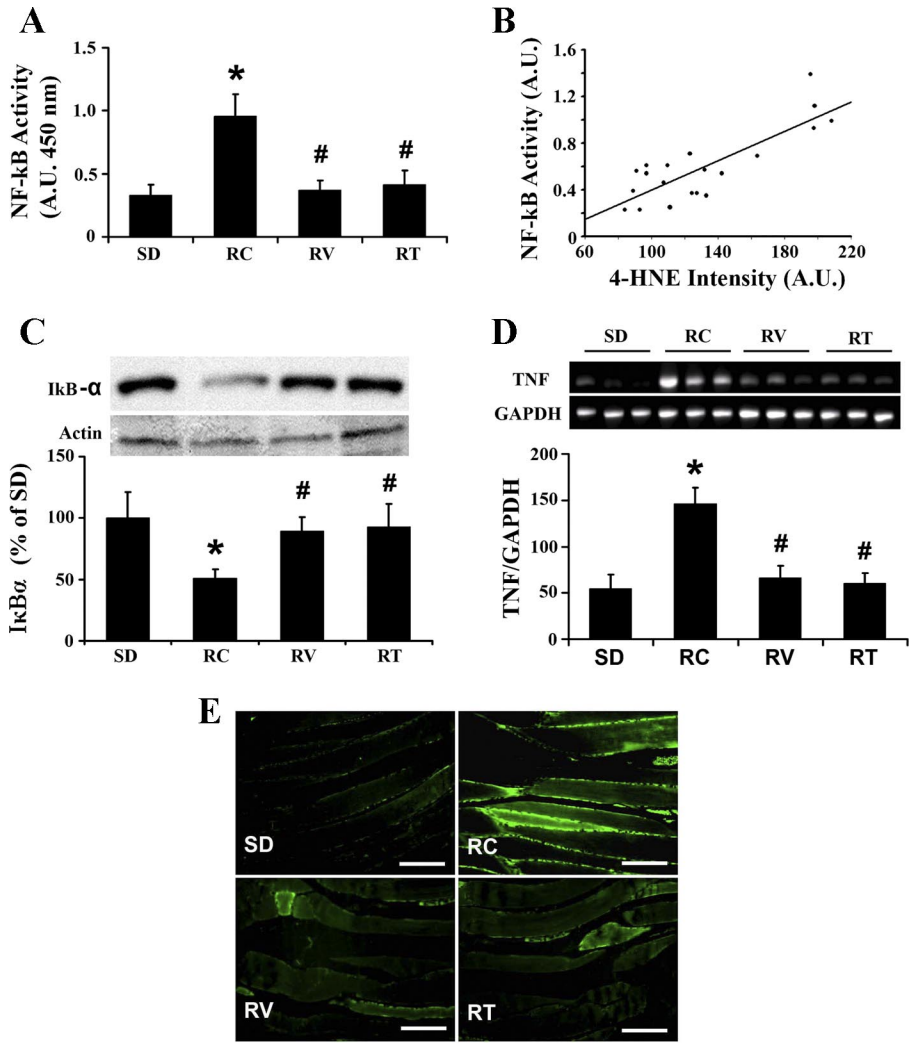

Fig. 2. NF-κB nuclear translocation and TNF-α expression in soleus muscle from Ren-2 rats. *A*: NoShift assay showing increased NF-κB p65 nuclear translocation in soleus muscle from Ren-2 compared with SD rats and blunted NF-κB p65 nuclear translocation in RV and RT groups. AU, arbitrary units. *B*: correlation between skeletal muscle NF-κB activities and 4-HNE staining intensities ($r = 0.786$, $P < 0.01$). *C*: cytosolic IκBα levels in soleus muscles from Ren-2 rats, including representative immunoblots with β-actin loading controls (*top*) and mean band densities compared with SD rats (*bottom*). *D*: RT-PCR for TNF-α mRNA expression normalized to GAPDH. *E*: representative photomicrographs showing increased TNF-α immunostaining (green) in Ren-2 rat soleus muscles. Values are means ± SE for 4–5 rats for each group. *$P < 0.05$ vs. SD. #$P < 0.05$ vs. RC. Magnification ×400. Scale bar 50 μm.

Increased TNF-α expression in soleus muscle from Ren-2 rats. NF-κB activation is known to upregulate inflammatory cytokines such as TNF-α (12), whereas TNF-α is a multifunctional cytokine that has been linked to insulin resistance (26). To determine whether NF-κB activation in skeletal muscle is associated with an increase in the inflammatory cytokine TNF-α, RT-PCR and immunostaining were performed. TNF-α mRNA and protein levels were greater in skeletal muscle from Ren-2 than SD rats (Fig. 2, *D* and *E*). Again, this effect was attenuated in Ren-2 soleus muscle treated with the AT_1R blocker valsartan or the superoxide scavenger tempol (Fig. 2, *D* and *E*).

ANG II-induced ROS activates NF-κB in L6 myotubes. The above-described in vivo results from Ren-2 rats suggest that increased ROS might mediate the ANG II-induced NF-κB activation expression in skeletal muscle. To further evaluate this possibility, L6 myoblasts were differentiated into myotubes and then treated with ANG II alone or ANG II plus each of the following: gp91 ds-tat (a specific NADPH inhibitor peptide that blocks $p47^{phox}$ binding to $gp91^{phox}$), valsartan (an AT_1R blocker), NAC (an antioxidant), or MG-132 (an NF-κB inhibitor). NF-κB p65 nuclear translocation and cytosolic IκBα were determined by NoShift assay and immunoblot, respectively. ANG II significantly increased NF-κB p65 nuclear translocation, and concomitant treatment with gp91 ds-tat, valsartan, NAC, or MG-132 inhibited ANG II-induced NF-κB p65 nuclear binding activity in L6 myotubes (Fig. 3*A*). Furthermore, when L6 myotubes were transfected with NF-κB p65 siRNA, not only was p65 subunit expression reduced (Fig. 3*B*), but NF-κB nuclear translocation in the presence of ANG II was significantly lower than when L6 myotubes were transfected with scrambled siRNA or treated with ANG II alone (Fig. 3*C*). NF-κB translocation with and without inhibitors was inversely associated with cytosolic IκB protein levels measured by Western blotting (data not shown).

ANG II-induced NF-κB activation mediated TNF-α production in L6 myotubes. ANG II induced TNF-α production in a dose-dependent manner that reached statistical significance at 10^{-7} M ANG II compared with untreated L6 myotubes (Fig. 4*A*). Alternatively, coadministration of valsartan, NAC, gp91 ds-tat, or MG-132 reversed ANG II-induced TNF-α production in L6 myotubes. Similarly, coadministration of the NF-κB inhibitor MG-132 (Fig. 4*B*) or transfection of NF-κB p65 siRNA (Fig. 4*C*) reversed ANG II-induced TNF-α production in the presence of ANG II. These findings suggest that increased TNF-α production by skeletal muscle in the presence of ANG II is mediated by ROS-induced NF-κB activation.

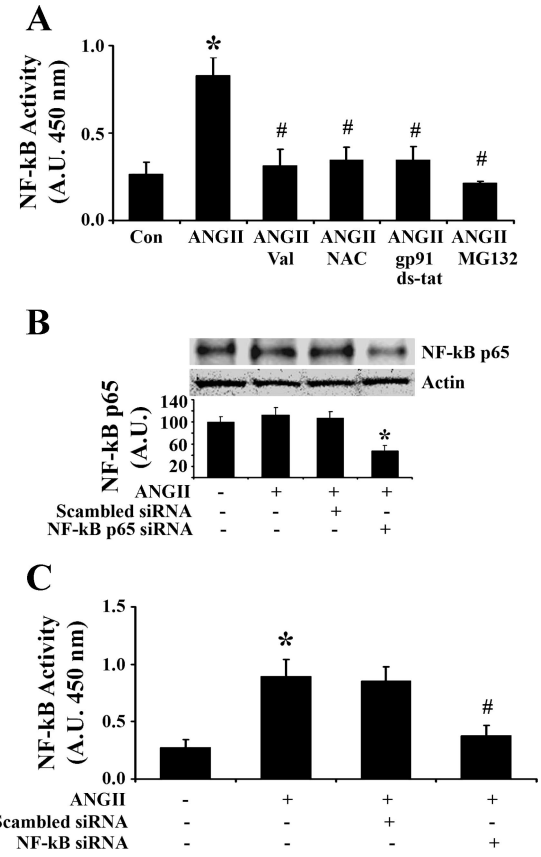

Fig. 3. NF-κB nuclear translocation in L6 myotubes. *A*: NF-κB nuclear translocation (activation) detected by NoShift assay. ANG II significantly induced NF-κB p65 nuclear translocation, which was prevented by the ANG II type 1 receptor (AT_1R) blocker valsartan (Val), the antioxidant *N*-acetylcysteine (NAC), the NADPH oxidase inhibitor peptide gp91 ds-tat, or the NF-κB inhibitor MG-132. $*P < 0.05$ vs. untreated control. $\#P < 0.05$ vs. ANG II alone. *B*: NF-κB p65 protein levels were not affected by ANG II alone or ANG II with scrambled RNA. Small interfering RNA (siRNA) targeting of NF-κB p65 subunit significantly decreased p65 protein levels in L6 myotubes compared with ANG II alone. $*P < 0.05$. *C*: NF-κB p65 siRNA significantly attenuated ANG II-induced NF-κB p65 nuclear translocation compared with scrambled RNA. $*P < 0.05$, ANG II alone vs. no treatment. $\#P < 0.05$, NF-κB p65 siRNA vs. ANG II alone. Values are means ± SE for 3 separate experiments with triplex wells for each group.

Inhibition of NF-κB improved insulin-mediated phosphorylation (Ser^{473}) of Akt and translocation of GLUT-4 in L6 myotubes. To determine whether activation of NF-κB mediates ANG II-induced insulin resistance in skeletal muscle, L6 myotubes were preincubated with valsartan, NAC, gp91 ds-tat, or the NF-κB inhibitor MG-132 for 1 h and then coincubated with ANG II for 24 h. Then the myotubes were exposed to insulin (100 nM) for 15 min. Phosphorylation (Ser^{473}) of Akt and translocation of GLUT-4 to PM were measured by Western blot (Fig. 5). In these experiments, ANG II reduced insulin-mediated phosphorylation (Ser^{473}) of Akt and translocation of GLUT-4. This inhibition was largely prevented by pretreatment with valsartan, NAC, gp91 ds-tat, or the NF-κB inhibitor MG-132 (Fig. 5, *A* and *B*), suggesting that ROS-induced NF-κB activation plays an important role in ANG II-induced skeletal muscle insulin resistance.

NF-κB p65 siRNA knockdown of p65 protein expression prevented ANG II inhibition of insulin signaling. To further confirm the role of NF-κB in ANG II-induced skeletal muscle insulin resistance, siRNA targeting NF-κB subunit p65 was employed in L6 myotubes. NF-κB p65 siRNA transfection significantly reduced NF-κB p65 levels and inhibited ANG II-induced NF-κB activation (Fig. 3, *B* and *C*) while also reversing decreases in insulin-stimulated phosphorylation (Ser^{473}) of Akt (Fig. 5*C*) and translocation of GLUT-4 in L6 myotube PM (Fig. 5*D*). GLUT-1 transporter levels, while detected in L6 myotube PM, were not altered by ANG II (data not shown).

DISCUSSION

The prevalence of the metabolic syndrome is steadily increasing. Hypertension and type 2 diabetes mellitus, two important manifestations of the metabolic syndrome, often coexist and frequently progress to cardiovascular disease. Insulin resistance plays a central role in the pathogenesis of the metabolic syndrome. This may be attributable in part to ANG II, which not only plays a pivotal role in the development of hypertension, but it also impairs insulin action on skeletal muscle via the AT_1R (25, 26). As the major tissue for insulin-mediated glucose disposal, skeletal muscle is particularly crucial in the development of insulin resistance. Skeletal muscle expresses many components of RAS, including AT_1R (26), and ANG II has direct effects on skeletal muscle that lead to insulin

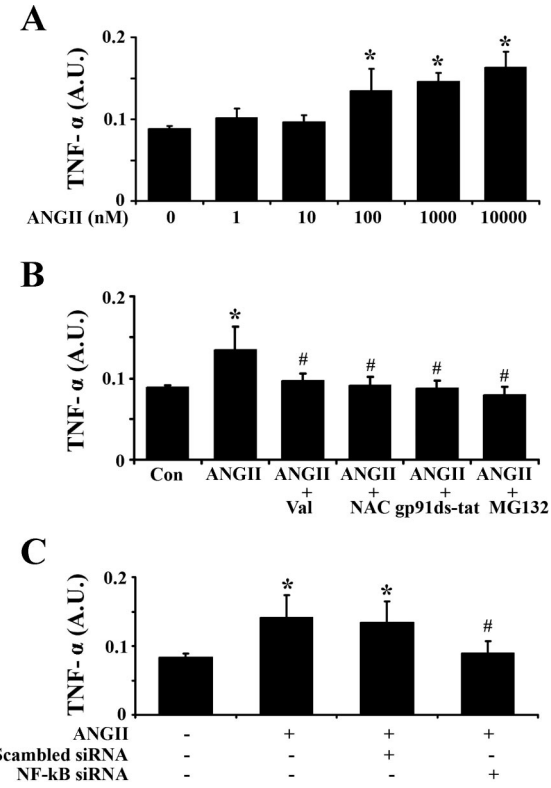

Fig. 4. ANG II-induced TNF-α production detected by ELISA in L6 myotubes. *A*: ANG II induced TNF-α production in a dose-dependent manner. $*P < 0.05$ vs. no treatment. *B*: inhibition of ANG II-induced increase in TNF-α production by the AT_1R blocker valsartan, the antioxidant NAC, the NADPH oxidase inhibitor gp91 ds-tat peptide, and the NF-κB inhibitor MG-132. $*P < 0.05$ vs. no treatment (Con). $\#P < 0.05$ vs. ANG II alone. *C*: significant reduction of L6 myotube TNF-α production in the presence of ANG II by NF-κB p65 siRNA, but not scrambled siRNA. $*P < 0.05$ vs. no treatment. $\#P < 0.05$ vs. ANG II alone. Values are means ± SE for 3 separate experiments with triplex wells for each group.

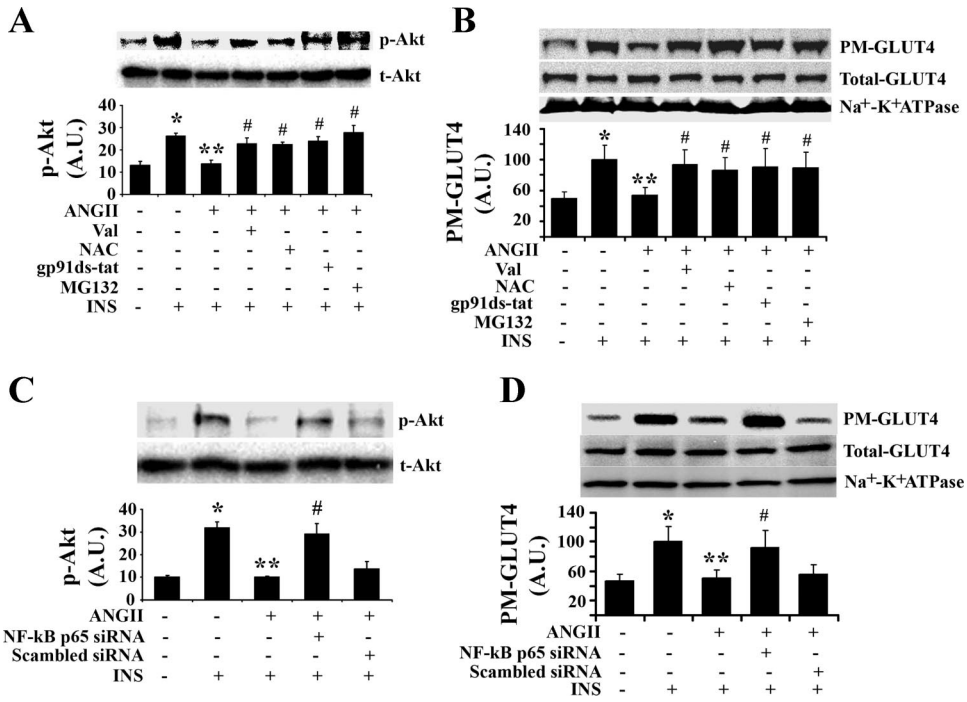

Fig. 5. Insulin-stimulated phosphorylation (Ser^{473}) of Akt and translocation of GLUT-4 to plasma membrane (PM) in L6 myotubes. Representative immunoblots and bar graphs indicating mean ± SE for insulin-mediated phosphorylation (Ser^{473}) of Akt (*A*) and translocation of GLUT-4 (*B*) in untreated L6 myotubes or myotubes treated with 10^{-7} M ANG II, with or without valsartan, NAC, gp91 ds-tat, or MG-132. *$P < 0.05$ vs. no treatment. **$P < 0.05$ vs. insulin (INS) alone. #$P < 0.05$ vs. ANG II + INS. *C* and *D*: knockdown of NF-κB p65 improved insulin-mediated phosphorylation (Ser^{473}) of Akt and translocation of GLUT-4 to the PM. *$P < 0.05$ vs. no treatment. **$P < 0.05$ vs. INS alone. #$P < 0.05$ vs. ANG II + INS. Values are means ± SE for 3 separate experiments with triplex wells for each group.

resistance (3, 22, 30). ANG II appears to induce insulin resistance at the levels of insulin receptor substrate-1 tyrosine phosphorylation (22), Akt activation, and/or distal to Akt activation, perhaps at the level of glucose transporter (GLUT-4) translocation (14). Nevertheless, this insulin resistance appears closely linked to an increase in oxidative stress (3, 14, 30). The intermediate steps linking ANG II-induced ROS to impaired insulin signaling in skeletal muscle remain uncertain.

The primary finding in this investigation is that ANG II-induced oxidative stress activates NF-κB in skeletal muscle, which in turn diminishes insulin signaling and GLUT-4 translocation. This interpretation is based on the following findings. *1*) ANG II-induced oxidative stress, NF-κB activation, and increased TNF-α were documented in skeletal muscle from insulin-resistant Ren-2 rats and ANG II-treated L6 myotubes. *2*) Antioxidant treatment inhibited ANG II-induced NF-κB activation and TNF-α production in Ren-2 skeletal muscle and L6 myotubes. *3*) ANG II inhibition of insulin-mediated Akt activation and GLUT-4 translocation in L6 myotubes was significantly attenuated by blockade of the AT_1R (valsartan), antioxidant treatment (NAC), NF-κB inhibition (MG-132), or NF-κB p65 knockdown (siRNA; Figs. 3 and 5). Multiple sources of increased ROS are possible, but NADPH oxidase remains a leading candidate, since pretreatment of L6 cells with the specific inhibitor gp91 ds-tat reduced NF-κB activation and improved GLUT-4 translocation in the presence of insulin. To our knowledge, this is the first study to document that NF-κB activation mediates ANG II-induced insulin resistance in skeletal muscle in an NADPH oxidase-dependent manner. NF-κB activation is known to promote increases in inflammatory cytokines, including TNF-α, which have been linked to insulin resistance. Interestingly, in the present study, ANG II-induced TNF-α generation in L6 myotube cultures was attenuated when the myotubes were preincubated with an antioxidant (NAC), an NADPH oxidase inhibitor (gp91 ds-tat), or an NF-κB inhibitor (MG-132) or previously transfected with NF-κB p65 siRNA (Fig. 4).

ANG II exerts prooxidant and proinflammatory effects that regulate cell growth, apoptosis, migration, inflammation, and fibrosis and impair insulin signaling in many tissues, including skeletal muscle (3, 17, 30). The ANG II effects on insulin signaling in skeletal muscle appear to be, at least in part, mediated by NADPH oxidase-derived ROS (30). ROS, in turn, may be an important intermediary between the ANG II/AT_1R binding event and several downstream cellular outcomes. However, little information as to how ROS diminishes insulin signaling has been garnered. ROS has been shown to activate several signaling pathways, including those involving redox-sensitive transcription factors (NF-κB, activating protein-1, and hypoxia inducible factor-1) (1, 27). NF-κB, in turn, stimulates the expression of numerous genes, including TNF-α and IL-6. It has also been shown that NF-κB is involved in fatty acid-induced insulin resistance in liver and adipocytes (5, 21). Furthermore, chronic inflammation and inflammatory cytokines, such as TNF-α, IL-6, and IL-8, may play a fundamental role in the pathogenesis of insulin resistance and type 2 diabetes mellitus (20). Some of the questions that have remained unanswered, particularly in skeletal muscle, include the following. *1*) Does ANG II induce NF-κB activation? *2*) If so, does NADPH oxidase-generated ROS mediate ANG II-induced NF-κB activation? *3*) Does NF-κB activation participate in ANG II-induced skeletal muscle insulin resistance? In the present study, skeletal muscle from insulin-resistant Ren-2 rats exhibited increased NF-κB activation and TNF-α production, which were reversed when the animals were treated with the AT_1R blocker valsartan or the superoxide scavenger tempol. Moreover, in vitro experiments confirmed that NF-κB activation was essential for perpetuation of ANG II-induced skeletal muscle insulin resistance, since NF-κB inhibition with MG-132 or NF-κB p65 knockdown by siRNA techniques prevented

ANG II-induced reductions in insulin-mediated Akt activation and GLUT-4 translocation.

Collectively, several novel findings were demonstrated in the present investigation. *1*) NF-κB activation and nuclear translocation are required for ANG II-induced insulin resistance in skeletal muscle. *2*) ANG II increased NF-κB activation and TNF-α production, which were dependent on NADPH oxidase-derived ROS. *3*) Blocking the AT_1R, inhibiting NADPH oxidase, or preventing NF-κB activation attenuated TNF-α increases in cultured myotubes. The data provide solid evidence indicating that NADPH oxidase-generated ROS activates NF-κB, thus linking ANG II, ROS, and insulin resistance in skeletal muscle. These findings may provide important insights into the pathogenesis and potential targets for treatment that might play a pivotal role in alleviating ANG II-induced insulin resistance.

GRANTS

This work was supported by National Heart, Lung, and Blood Institute Grant R01-HL-073101-02, Veterans Affairs Merit Award 0018, and Novartis Pharmaceuticals (J. R. Sowers) and Department of Veterans Affairs Veterans Integrated Service Network 15 and Advanced Research Career Development Awards (C. S. Stump).

REFERENCES

1. **Baldwin AS Jr.** The transcription factor NF-κB and human disease. *J Clin Invest* 107: 3–6, 2001.
2. **Bays H, Mandarino L, DeFronzo RA.** Role of the adipocyte, free fatty acids, and ectopic fat in pathogenesis of type 2 diabetes mellitus: peroxisomal proliferator-activated receptor agonists provide a rational therapeutic approach. *J Clin Endocrinol Metab* 89: 463–478, 2004.
3. **Blendea MC, Jacobs D, Stump CS, McFarlane SI, Ogrin C, Bahtyiar G, Stas S, Kumar P, Sha Q, Ferrario CM, Sowers JR.** Abrogation of oxidative stress improves insulin sensitivity in the Ren-2 rat model of tissue angiotensin II overexpression. *Am J Physiol Endocrinol Metab* 288: E353–E359, 2005.
4. **Browning JD, Horton JD.** Molecular mediators of hepatic steatosis and liver injury. *J Clin Invest* 114: 147–152, 2004.
5. **Cai D, Yuan M, Frantz DF, Melendez PA, Hansen L, Lee J, Shoelson SE.** Local and systemic insulin resistance resulting from hepatic activation of IKK-β and NF-κB. *Nat Med* 11: 183–190, 2005.
6. **Esterbauer H, Schaur RJ, Zollner H.** Chemistry and biochemistry of 4-hydroxynonenal, malonaldehyde and related aldehydes. *Free Radic Biol Med* 11: 81–128, 1991.
7. **Forbes JM, Cooper ME, Thallas V, Burns WC, Thomas MC, Brammar GC, Lee F, Grant SL, Burrell LA, Jerums G, Osicka TM.** Reduction of the accumulation of advanced glycation end products by ACE inhibition in experimental diabetic nephropathy. *Diabetes* 51: 3274–3282, 2002.
8. **Ford ES, Giles WH, Dietz WH.** Prevalence of the metabolic syndrome among US adults: findings from the Third National Health and Nutrition Examination Survey. *JAMA* 287: 356–359, 2002.
9. **Henriksen EJ, Jacob S, Kinnick TR, Teachey MK, Krekler M.** Selective angiotensin II receptor antagonism reduces insulin resistance in obese Zucker rats. *Hypertension* 38: 884–890, 2001.
10. **Kamata H, Manabe T, Oka S, Kamata K, Hirata H.** Hydrogen peroxide activates IκB kinases through phosphorylation of serine residues in the activation loops. *FEBS Lett* 519: 231–237, 2002.
11. **Mitsumoto Y, Burdett E, Grant A, Klip A.** Differential expression of the GLUT1 and GLUT4 glucose transporters during differentiation of L6 muscle cells. *Biochem Biophys Res Commun* 175: 652–659, 1991.
12. **Muller DN, Dechend R, Mervaala EM, Park JK, Schmidt F, Fiebeler A, Theuer J, Breu V, Ganten D, Haller H, Luft FC.** NF-κB inhibition ameliorates angiotensin II-induced inflammatory damage in rats. *Hypertension* 35: 193–201, 2000.
13. **Nathan C.** Specificity of a third kind: reactive oxygen and nitrogen intermediates in cell signaling. *J Clin Invest* 111: 769–778, 2003.
14. **Ogihara T, Asano T, Ando K, Chiba Y, Sakoda H, Anai M, Shojima N, Ono H, Onishi Y, Fujishiro M, Katagiri H, Fukushima Y, Kikuchi M, Noguchi N, Aburatani H, Komuro I, Fujita T.** Angiotensin II-induced insulin resistance is associated with enhanced insulin signaling. *Hypertension* 40: 872–879, 2002.
15. **Otogawa K, Kinoshita K, Fujii H, Sakabe M, Shiga R, Nakatani K, Ikeda K, Nakajima Y, Ikura Y, Ueda M, Arakawa T, Hato F, Kawada N.** Erythrophagocytosis by liver macrophages (Kupffer cells) promotes oxidative stress, inflammation, and fibrosis in a rabbit model of steatohepatitis: implications for the pathogenesis of human nonalcoholic steatohepatitis. *Am J Pathol* 170: 967–980, 2007.
16. **Peraldi P, Spiegelman B.** TNF-α and insulin resistance: summary and future prospects. *Mol Cell Biochem* 182: 169–175, 1998.
17. **Rajagopalan S, Kurz S, Munzel T, Tarpey M, Freeman BA, Griendling KK, Harrison DG.** Angiotensin II-mediated hypertension in the rat increases vascular superoxide production via membrane NADH/NADPH oxidase activation. Contribution to alterations of vasomotor tone. *J Clin Invest* 97: 1916–1923, 1996.
18. **Rey FE, Cifuentes ME, Kiarash A, Quinn MT, Pagano PJ.** Novel competitive inhibitor of NAD(P)H oxidase assembly attenuates vascular O_2^- and systolic blood pressure in mice. *Circ Res* 89: 408–414, 2001.
19. **Richey JM, Ader M, Moore D, Bergman RN.** Angiotensin II induces insulin resistance independent of changes in interstitial insulin. *Am J Physiol Endocrinol Metab* 277: E920–E926, 1999.
20. **Shoelson SE, Lee J, Goldfine AB.** Inflammation and insulin resistance. *J Clin Invest* 116: 1793–1801, 2006.
21. **Sinha S, Perdomo G, Brown NF, O'Doherty RM.** Fatty acid-induced insulin resistance in L6 myotubes is prevented by inhibition of activation and nuclear localization of nuclear factor κB. *J Biol Chem* 279: 41294–41301, 2004.
22. **Sloniger JA, Saengsirisuwan V, Diehl CJ, Dokken BB, Lailerd N, Lemieux AM, Kim JS, Henriksen EJ.** Defective insulin signaling in skeletal muscle of the hypertensive TG(mREN2)27 rat. *Am J Physiol Endocrinol Metab* 288: E1074–E1081, 2005.
23. **Sowers JR.** Hypertension, angiotensin II, and oxidative stress. *N Engl J Med* 346: 1999–2001, 2002.
24. **Stephens L, Anderson K, Stokoe D, Erdjument-Bromage H, Painter GF, Holmes AB, Gaffney PR, Reese CB, McCormick F, Tempst P, Coadwell J, Hawkins PT.** Protein kinase B kinases that mediate phosphatidylinositol 3,4,5-trisphosphate-dependent activation of protein kinase B. *Science* 279: 710–714, 1998.
25. **Stump CS, Hamilton MT, Sowers JR.** Effect of antihypertensive agents on the development of type 2 diabetes mellitus. *Mayo Clin Proc* 81: 796–806, 2006.
26. **Stump CS, Henriksen EJ, Wei Y, Sowers JR.** The metabolic syndrome: role of skeletal muscle metabolism. *Ann Med* 38: 389–402, 2006.
27. **Tak PP, Firestein GS.** NF-κB: a key role in inflammatory diseases. *J Clin Invest* 107: 7–11, 2001.
28. **Taniyama Y, Hitomi H, Shah A, Alexander RW, Griendling KK.** Mechanisms of reactive oxygen species-dependent downregulation of insulin receptor substrate-1 by angiotensin II. *Arterioscler Thromb Vasc Biol* 25: 1142–1147, 2005.
29. **Torlone E, Britta M, Rambotti AM, Perriello G, Santeusanio F, Brunetti P, Bolli GB.** Improved insulin action and glycemic control after long-term angiotensin-converting enzyme inhibition in subjects with arterial hypertension and type II diabetes. *Diabetes Care* 16: 1347–1355, 1993.
30. **Wei Y, Sowers JR, Nistala R, Gong H, Uptergrove GM, Clark SE, Morris EM, Szary N, Manrique C, Stump CS.** Angiotensin II-induced NADPH oxidase activation impairs insulin signaling in skeletal muscle cells. *J Biol Chem* 281: 35137–35146, 2006.
31. **Yusuf S, Sleight P, Pogue J, Bosch J, Davies R, Dagenais G.** Effects of an angiotensin-converting enzyme inhibitor, ramipril, on cardiovascular events in high-risk patients. The Heart Outcomes Prevention Evaluation Study Investigators. *N Engl J Med* 342: 145–153, 2000.
32. **Zhang M, Kho AL, Anilkumar N, Chibber R, Pagano PJ, Shah AM, Cave AC.** Glycated proteins stimulate reactive oxygen species production in cardiac myocytes: involvement of Nox2 (gp91phox)-containing NADPH oxidase. *Circulation* 113: 1235–1243, 2006.